Energy & Environmental Science

Cite this: *Energy Environ. Sci.*, 2011, **4**, 1813

www.rsc.org/ees

PAPER

High–rate electrochemical capacitors from highly graphitic carbon–tipped manganese oxide/mesoporous carbon/manganese oxide hybrid nanowires†

Hao Jiang,[ab] Liping Yang,[b] Chunzhong Li,*[a] Chaoyi Yan,[c] Pooi See Lee[c] and Jan Ma[bc]

Received 12th January 2011, Accepted 4th March 2011
DOI: 10.1039/c1ee01032h

In this paper, using manganese oxide as an example, we report the successful design and synthesis of a novel one-dimensional highly graphitic carbon-tipped manganese oxide/mesoporous carbon/manganese oxide hybrid nanowire. The unique structure significantly improves the conductivity of metal oxide materials, which is a key limitation in pseudocapacitors. The hybrid nanowire with optimal carbon content, when applied as an electrode, exhibits superior capacitive properties in 1 M Na_2SO_4 aqueous solution, such as high specific capacitance (266 F g^{-1} at 1 A g^{-1}), excellent rate capability (56.4% capacity retention at 60 A g^{-1}) and outstanding cycling stability (without degradation after 1200 cycles). The energy densities achieved can be as high as 20.8 W h kg^{-1}, at a power density of 30 kW kg^{-1}. The results demonstrated that the manganese oxide in our hybrid nanomaterial was efficiently utilized with the assistance of the highly conductive graphitic carbon-tipped mesoporous carbon shell. It is reckoned that the present low-cost novel hybrid nanowire can serve as a promising electrode material for supercapacitors and other electrochemical devices.

1. Introduction

The increasing demand on environmentally friendly, high-performance energy storage systems has stimulated intense research interest in areas such as batteries and capacitors. Supercapacitors have emerged as one of the most promising candidates for energy storage as they can provide a higher power density than batteries, and a higher energy density than conventional dielectric capacitors.[1–3] They have extensive applications, including consumer electronics, energy management, memory back-up systems, industrial power and mobile electrical systems.[4] In these applications, it is well accepted that the improvement of power density and energy density, as well as low fabrication costs,[5,6] are the essential criteria. In the search for an appropriate material for supercapacitor electrodes, various transition metal oxides,[7,8] carbonaceous materials[9,10] and conducting polymers[11,12] have been explored. Among them, manganese oxide is considered to be one of the most promising transition metal oxides for next generation supercapacitors due to its low cost, environmental benignity, ideal capacitor performance and high safety during operations.[13–15]

Despite the theoretical expectation that electrodes made from manganese oxide should exhibit high specific capacitance and rate capability,[5,16,17] poor cycling stability and rate capability have limited its performance in practical applications. It is noted that one-dimensional (1D) nanostructures with controlled size, crystallinity and chemical composition could be designed to achieve

[a]*Key Laboratory for Ultrafine Materials of Ministry of Education, School of Materials Science and Engineering, East China University of Science & Technology, Shanghai, 200237, China. E-mail: czli@ecust.edu.cn; Fax: +86- 21- 6425- 0624; Tel: +86- 21- 6425- 0949*
[b]*Temasek Laboratories, Nanyang Technological University, Singapore, 637553, Singapore*
[c]*School of Materials Science and Engineering, Nanyang Technological University, Singapore, 639798, Singapore*

† Electronic supplementary information (ESI) available: SEM images, XRD patterns, TGA, CV and CD curves. See DOI: 10.1039/c1ee01032h

Broader context

Supercapacitors have emerged as a promising candidate for energy storage as they can provide a higher power density than batteries, and a higher energy density than conventional dielectric capacitors. Many materials have been investigated as the electrode materials in supercapacitors. Among them, transition metal oxides are considered as one of the most promising candidates. However, poor conductivity has limited their high specific capacitance potential in practical applications. To overcome this weakness, a novel architecture has been proposed in the present work. Using manganese oxide as an example, highly graphitic carbon-tipped manganese oxide/mesoporous carbon/manganese oxide hybrid nanowire has been successfully designed and synthesized, which significantly improved the conductivity of the manganese oxide.

faster redox reactions, higher specific surface areas and shorter diffusion paths for electrons and ions.[18–20] Nevertheless, conductivity of these 1D nanowires still needs further improvement to meet the requirements of supercapacitors with high energy and power densities.

In recent years, coaxial nanowires, such as metal oxide/conducting polymers, [17,21,22] and metal oxide/CNTs,[5,23,24] have attracted great interest due to their synergistic properties obtained by combining different materials. However, metal oxide/conducting polymers coaxial materials suffer from mechanical instability or poor cycle ability.[21,25] On the other hand, for composites with carbonaceous materials, including CNTs, carbon foam, and activated carbon, metal oxides exhibit a pronounced increase in performance only when a small amount of metal oxide is incorporated in the carbonaceous materials.[26–28] However, it is noted that for practical applications, such as electric vehicles, high metal oxide concentrations in the electrodes are needed.[25,29] Thus far, there have been limited reports on composite electrodes with good capacitive behavior and a high loading of transition metal oxides without the use of CNTs. This is because only a thin layer of the oxide material participates in the charge storage process. As more manganese oxide is incorporated, the redox activity of manganese oxide quickly decreases due to the lower utilization of active materials, leading to a significant degradation of capacitive performance.

Furthermore, the introduction of CNTs increases the fabrication cost and hence restricts the composite's potential development. Therefore, it is highly desirable to enhance rate capability with a high specific capacitance while maintaining a low fabrication cost, especially in cases where high metal oxide loading is needed.

In the present paper, new insight on the design of an ideal supercapacitor with both high energy and power densities is provided. With manganese oxide as an example, for the first time, we have designed and synthesized a novel 1D highly graphitic carbon-tipped manganese oxide/mesoporous carbon/manganese oxide hybrid nanostructure (labeled as MMCM hybrid nanowires, see Experimental section) for high performance electrode material, as illustrated in Fig. 1. The designed hybrid nanowire is different from the traditional structure due to the loading of metal oxide on the surface of carbon materials. The unique structure possesses several major advantages: (1) the carbon layer coated on the surface of the MnO_2 nanowire overcomes the poor conductivity of metal oxide; (2) the mesoporous nature of the carbon shell ensures interaction between the electrolyte and the active inner materials; (3) the small manganese oxide nanoparticles dispersed on the surface of the mesoporous carbon nanotubes can be almost fully utilized for the enhancement of capacitive performance. Furthermore, the highly graphitic carbon is introduced because it fully accessible to ion adsorption with excellent conductivity.[30,31] The hybrid nanowire with 50.6% carbon content has been observed to exhibit the best capacitive performance. This result has shown that this novel hybrid nanostructure provides a new route to design and synthesize future electrode materials for high-performance supercapacitor applications.

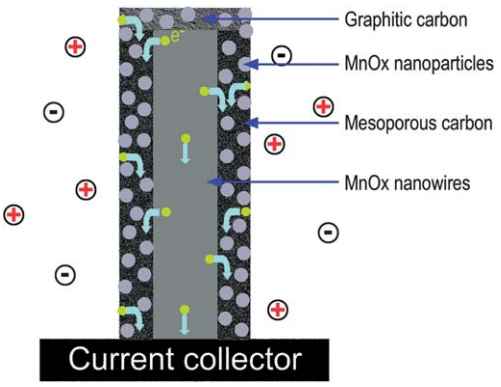

Fig. 1 Schematic image of the highly graphitic carbon-tipped manganese oxide/mesoporous carbon/manganese oxide hybrid nanowires. The mesoporous carbon supplies a direct path for electrons and allows free ion insertion/extraction.

2. Experimental details

All the reagents used in the experiments were analytical grade (purchased from Sigma-Aldrich) and used without further purification.

2.1. Synthesis of MnO_2 nanowires

$Mn(NO_3)_2 \cdot 4H_2O$ (0.2685 g) and sodium dodecyl benzene sulfonate (SDBS, 0.3845 g) were first dissolved in 30 mL of deionized water. When the solution turned clear, $KMnO_4$ (0.2 M, 5 mL) was added to the above solution with continuous stirring for about 30 min. The resulting cloudy solution was transferred into a 50 mL Teflon-lined stainless steel autoclave, then heated at 180 °C for 4–6 h, followed by natural cooling to room temperature. The precipitates, *i.e.* MnO_2 nanowires, were collected by filtration, washed with deionized water and absolute ethanol, and finally dried at 60 °C for 6 h.

2.2. Synthesis of highly graphitic carbon-tipped manganese oxide/mesoporous carbon/manganese oxide hybrid nanowires

Dopamine was used for the coating on the as-synthesized MnO_2 nanowires according to ref. 32. The triblock copolymer PEO-PPO-PEO (P123) was used as a structure-directing agent for generating the mesoporous phases. For a typical procedure, 40 mg of the above as-synthesized MnO_2 nanowires, 40 mg of P123 and 50 mg of 2-amino-2-hydroxymethyl-propane-1,3-diol (Tris) were dissolved and dispersed in 40 mL deionized water by subjecting it to about 10 min sonication, and then cooled down to room temperature. Subsequently, 80 mg dopamine was added to the mixture under stirring. The mixture was subjected to continuous magnetic stirring at room temperature for about 5 h. After that, the precipitates, *i.e.* polydopamine/manganese oxide, were collected by filtration, then washed several times with absolute ethanol, and then finally re-dispersed in isopropanol (50 mL). The coating thickness of the polydopamine layer can be tuned by varying the dopamine concentration or the polymerization time. Subsequently, the slurry was heated to approximately 83 °C in a water-cooled condenser with vigorous stirring, and $Mn(NO_3)_2 \cdot 4H_2O$ (100 mg) dissolved in 10 mL of deionized water was added rapidly into the above boiling solution. After refluxing for 2 h, the precipitates were then centrifuged, washed, and dried overnight in air at 60 °C. Finally, the resulting products were carbonized into highly graphitic carbon-tipped manganese oxide/

mesoporous carbon/manganese oxide hybrid nanowires (labeled as MMCM hybrid nanowires in subsequent text) under flowing argon at 850 °C for 2 h. For comparison, the manganese oxide/carbon/manganese oxide hybrids were synthesized using the same procedure, only without the addition of P123 (labeled as MCM hybrid nanowires in subsequent text).

2.3. Characterization

The as-prepared products were characterized with an X-ray powder diffractometer (XRD; Shimadzu XRD-6000, Cu Kα radiation) at a scan rate of 2 °C min^{-1}, scanning electron microscopy (FESEM; JEOL, JSM-7600F) equipped with an energy dispersive X-ray spectrometer (EDX), and transmission electron microscopy (TEM; JEOL, JEM-2100F) operated at 200 kV. N_2 adsorption/desorption was determined by Brunauer–Emmet–Teller (BET) measurements using an ASAP-2020 surface area analyzer. Thermogravimetric analysis (TGA, Q500) was carried out with a heating rate of 10 °C min^{-1} under flowing nitrogen.

2.4. Electrochemical measurements

The electrochemical measurements (Autolab PGSTAT30 potentiostat) were conducted using a three-electrode mode in a 1 M Na_2SO_4 solution. The working electrodes were prepared by mixing the active materials (80 wt.%) with acetylene black (15 wt. %), and polytetrafluoroethylene (PTFE, 5 wt.%). A small amount of absolute ethanol was then added to those mixtures to promote homogeneity. The mixture was coated onto the graphite paper (1 cm^2) to form the electrode layer by drying at 80 °C for a few hours. The reference electrode and counter electrode were Ag/AgCl electrode and platinum foil, respectively. Typical CV curves were measured between −0.1 and 0.9 V.

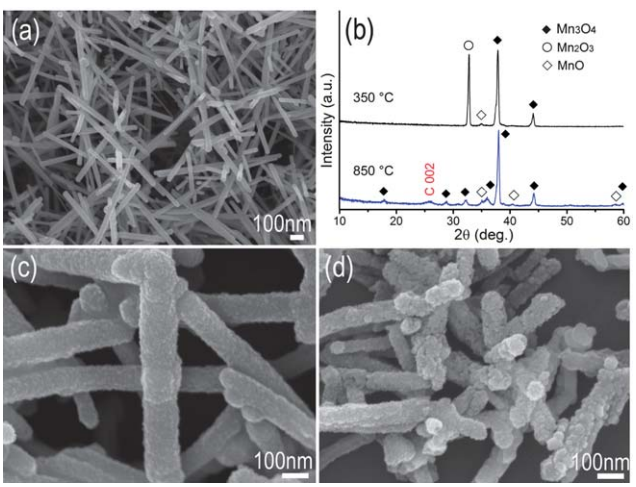

Fig. 2 (a) SEM image of the as-synthesized α–MnO_2 nanowires. (b) XRD patterns of the manganese oxide/polydopamine/manganese oxide carbonized at 350 °C (black line) and 850 °C (blue line) in flowing argon. (c, d) SEM images of the manganese oxide/polydopamine/manganese oxide before and after carbonization, respectively, at 850 °C under flowing argon.

3. Results and discussion

Fig. 2a shows the uniform MnO_2 nanowires with an average diameter of ~25 nm and a length of ~770 nm, synthesized by the simple surfactant-assisted hydrothermal method. The XRD pattern is provided in the ESI† (Fig. S1). Then, a layer of polymer was coated onto the MnO_2 nanowire surfaces by a dopamine self-polymerization process. It is noted that dopamine can form an adherent polydopamine coating on a wide variety of materials after self-polymerization in air.[32] In addition, polydopamine can keep nearly 54% of the weight during carbonization process, and withstand up to 800 °C in an inert atmosphere, according to the TG curves (Fig. S2, ESI†). This new finding offers us a novel approach that it is a feasible way of coating a layer of carbon onto the as-synthesized manganese oxide nanowires. During the polymerization process, the triblock copolymer PEO-PPO-PEO (P123) was used as a structure-directing agent to generate the mesoporous structures. In addition, it has been reported that polydopamine has substantial functional groups, which can react easily with Mn^{2+} to form Mn-based compounds.[32] After carbonization at 850 °C for 2 h in flowing argon, highly graphitic carbon-tipped manganese oxide/mesoporous carbon/manganese oxide hybrid nanowires are obtained, labeled as MMCM hybrid nanowires. The corresponding XRD pattern is shown in Fig. 2b, as a blue line. The peaks can be mainly assigned to the hausmannite Mn_3O_4 (JCPDS 24-0743) phase. The presence of the cubic MnO (◇) is indicated by the peaks at 35.0°, 40.5° and 58.7°, which is in good agreement with the literature (JCPDS, file No.: 89-2804). These results revealed that annealed MnO_2 underwent a phase transition in the inert atmosphere.[33] Accordingly, an additional peak at 26.0° is observed in Fig. 2b which was attributed to the (002) plane of the hexagonal graphite structure, suggesting the presence of highly graphitic carbon. The hybrid nanowires synthesized by the same procedure, simply without the addition of P123, exhibit almost the same XRD pattern, and were labeled as MCM hybrid nanowires. For comparison, the manganese oxide/polydopamine/manganese oxide hybrid nanowires were annealed at 350 °C for 2 h in flowing argon to remove the surfactant P123. The XRD pattern is shown in Fig. 2b, as a black line. No graphite peak was observed. The strong peak at 32.9° (○) was attributed to the (222) planes of cubic Mn_2O_3 (JCPDS, file No.: 89-2809), which were completely converted into Mn_3O_4 after annealing at 850 °C. The high-magnification SEM images of manganese oxide/polydopamine/manganese oxide hybrid nanowires before and after carbonization are shown in Fig. 2c and d, respectively. It can be seen that the hybrid nanowires possessed average diameters of ~110 nm before carbonization, and the diameter decreased to ~75 nm with rougher surfaces after carbonization. Most importantly, the MMCM hybrid nanowires maintained the original 1D morphology. After carbonization at 850 °C, the thickness of the carbon layer was estimated to be ~25 nm. The carbon content is ~50.6% according to the TGA result (Fig. S4, ESI†).

Detailed structural information of the MMCM hybrid nanowires was obtained using TEM. From a low magnification TEM image (Fig. 3a), it is clear that a layer of carbon is uniformly coated on the surface of the manganese oxide nanowires. In addition, the manganese oxide nanoparticles distribute on the surface of the mesoporous carbon with relative uniformity. These particles are crystalline, as confirmed by the circles marked in Fig. 3c and e. It should be pointed out that the interaction between the nanoparticles and

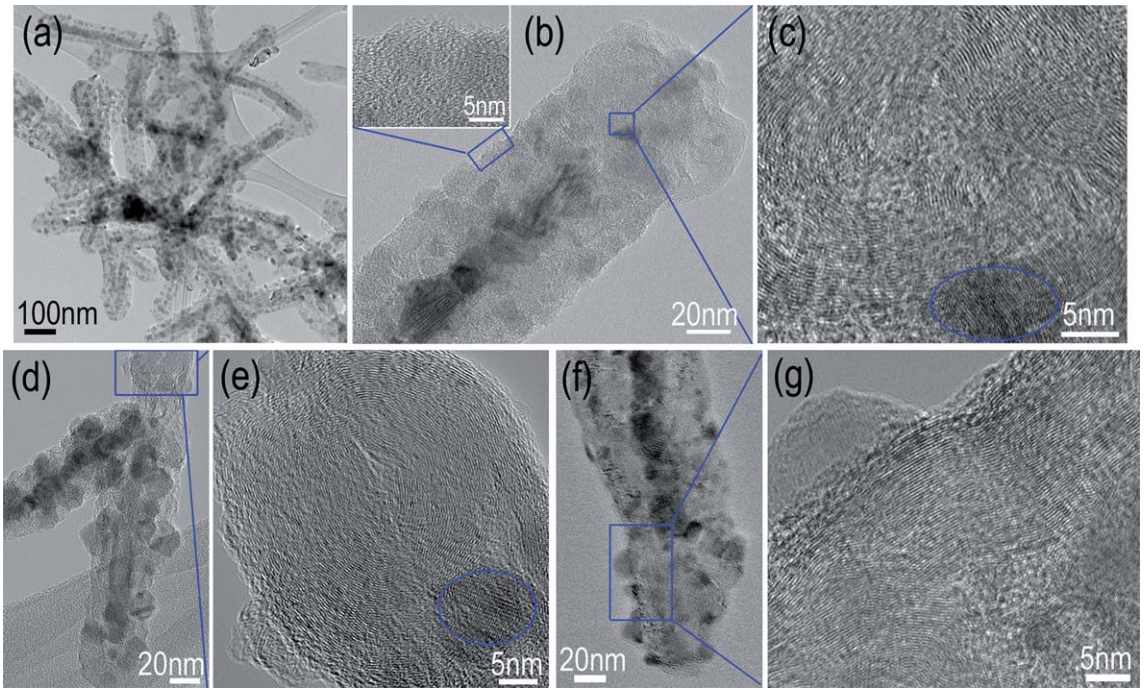

Fig. 3 (a) Low magnification and (b, d) high magnification TEM images of the MMCM hybrid nanowires. The inset of (b) is the high resolution TEM image taken from the corresponding blue boxed area. (c, e) High resolution TEM images of the MMCM hybrid nanowires. (f) High magnification and (g) high resolution TEM images of the MCM hybrid nanowires, respectively. The circles marked in (c, e) are the manganese oxide particles.

the carbon layer was very strong, supported by the fact that the nanoparticles could not be removed through washing, severe agitation and prolonged sonication. The hybrid nanowires have diameters of ~75 nm, which are in good agreement with the SEM results. High magnification TEM images further proved that the thickness of the carbon layer, as shown in Fig. 3b and d. Interestingly, the hybrid nanowires are tipped with highly graphitic carbon. The curved lattice fringes clearly show graphitic (002) layers with an interplanar spacing of 0.33 nm, which are consistent with the XRD result. The slight distortion of circular stripes (Fig. 3c) is attributed to defect formed during the graphitization process.[34] Furthermore, the tips of some nanowires are merged together, also forming highly graphitic carbon (Fig. 3d and e). It is noted that the highly graphitic carbon tips grew on the ends of the hybrid nanowires, rather than being physically placed on the end surface of the as-synthesized nanowires. More nanowires can be linked together to form a network structure, which will further accelerate the electronic transport and result in better electrochemical performances. On the sides of the hybrid nanowires, the carbon layer mainly exhibits a disordered mesoporous structure, as shown in the inset of Fig. 3b. These features are anticipated to be very beneficial for capacitive performance. To illustrate the role of P123, the MCM hybrid nanowires were also investigated by TEM (Fig. 3f and g). It can be seen that the carbon layer is mainly composed of highly graphitic carbon layers both at the tip and the two sides of the hybrid nanowires, suggesting that the addition of P123 contributes to the formation of the mesoporous structure.

The MMCM hybrid nanowire also shows a higher BET surface area of 137 $m^2\ g^{-1}$ than the MCM hybrid nanowires (75 $m^2\ g^{-1}$) and the pristine manganese oxide nanowires (71 $m^2\ g^{-1}$). The nitrogen adsorption and desorption isotherm and the pore size distribution are shown in Fig. 4. A distinct hysteresis loop can be observed in the larger range of *ca.* 0.45–1.0 P/P_0, which suggests the presence of a mesoporous structure.[35,36] It is obvious that the improvement of the specific surface area is mainly attributed to the formation of a mesoporous structure. The pore size distribution, calculated from desorption data using the BJH model, was evaluated to have an average of ~3.8 nm. The high BET surface area and mesoporous structure of the MMCM hybrid nanowires provides the possibility of efficient transport of electrons and ions in the electrode, hence leading to enhanced electrochemical capacity.

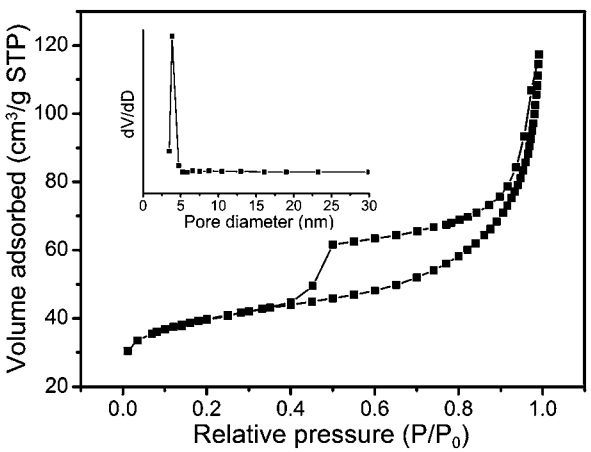

Fig. 4 Nitrogen adsorption and desorption isotherms and pore size distribution curves (inset) of the MMCM hybrid nanowires.

To explore the energy storage applications of this novel hybrid nanostructure, the sample was fabricated into a supercapacitor electrode, and the performance was evaluated with cyclic voltammogram (CV) and galvanostatic charge-discharge (CD) measurements. Fig. 5a shows the CV curves of the MMCM hybrid nanowires, the MCM hybrid nanowires, and the pristine MnO_2 nanowires recorded at a scan rate of 10 mV s^{-1}. The rectangular and symmetric CV curves show the ideal pseudocapacitive nature with fast charge/discharge processes. The MMCM hybrid nanowires exhibit a specific capacitance, as high as 226 F g^{-1}, while the capacitance for the MCM nanowires and the pristine MnO_2 nanowires are 164 F g^{-1} and 130 F g^{-1}, respectively. We then subjected the MMCM hybrid nanomaterials to further CV investigation under different scan rates, as shown in Fig. 5b. At a higher scan rate of 50 mV s^{-1}, the specific capacitance of the MMCM hybrid nanowires is 191 F g^{-1}. It is noted that even at a high scan rate of 500 mV s^{-1}, the MMCM nanowires manage to retain a capacitance of 114 F g^{-1}, suggesting that such high specific capacitance can be maintained under very high power operation.

Galvanostatic charge–discharge measurements were also carried out on the MMCM hybrid nanowires at different current densities, and the results are shown in Fig. 5c. It can be seen that the charging curves are symmetrical to their corresponding discharge counterparts. The specific capacitance is calculated from the discharge curves (see the ESI† for more details). At a low current density of 1 A g^{-1}, the specific capacitance can reach as high as 266 F g^{-1}, which is much higher than the pristine MnO_2 nanowires (157 F g^{-1}). The results are in good agreement with that of the CV characterization. It is well accepted that rate capability is an important factor for supercapacitors in high power applications. Fig. 5d shows the specific capacitance as a function of current density for the MMCM nanowires (red lines), the MCM nanowires (blue lines) and the pristine MnO_2 nanowires (black lines). It can be seen that the MMCM hybrid nanowires not only deliver high specific capacitance, but also maintain it at a high current density compared to the other two materials. As shown in Fig. 5d, a capacitance of 150 F g^{-1} (~56.4% retention) was retained at a current density as high as 60 A g^{-1}. To the best of our knowledge, this capability is comparable or superior to the best results reported for manganese oxide based materials in the literature. It was reported that manganese oxide nanoflower/carbon nanotube array (CNTA) composite electrodes presented an excellent rate capability, where 50.8% capacity retention at a current density of 77 A g^{-1} was achieved.[5] However, the specific capacitance of the composite was measured to be 199 F g^{-1} at low current density, and in addition, the use of CNTA increased the cost greatly, limiting its commercial potential. Furthermore, the specific capacitance of our material is also higher than that of other MnO_2-based composite materials reported thus far, such as that of MnO_2/multi-walled carbon nanotube composites (179 F g^{-1} at 5 mV s^{-1}),[37] CNT/carbon microfiber/MnO_2 composites (180 F g^{-1} at 10 mV s^{-1})[38] and graphene oxide-MnO_2 nanocomposites (111 F g^{-1} at 1 A g^{-1}).[39] Very recently, Li *et al.*[40] reported the synthesis of coaxially coated manganese oxide on vertically aligned carbon nanofiber arrays, which exhibited a specific capacitance as high as 320 F g^{-1} at ~1 A g^{-1}, but only 70 F g^{-1} at a high current density of ~15 A g^{-1}. In addition, MnO_2 nanoparticles enriched in poly(3,4-ethylenedioxythiophene) nanowires fabricated by Lee *et al.*[22] have also show a high specific capacitance (250 F g^{-1} at 5 mA cm^{-2}). However, these material systems showed a poor stability (10% loss after 500 cycles). The results demonstrate that our materials, showing a higher specific capacitance, and better rate capability with a low-cost fabrication, are expected to have a significant impact in the community.

Fig. 6 shows the Ragone plot (power density *vs.* energy density) of the MMCM hybrid nanowires (red line), the MCM hybrid nanowires (blue line) and the pristine MnO_2 nanowires (black line). The energy and power densities were derived from charge–discharge curves at different current densities. The MMCM hybrid nanowires delivered a high energy density of 26.9 W h kg^{-1} at a power density of 10 kW kg^{-1}, which is about 2.5 times larger than that of the pristine MnO_2 nanowires. More importantly, the MMCM hybrid nanowires can maintain a higher power density without a large sacrifice of energy density. Even at a power density

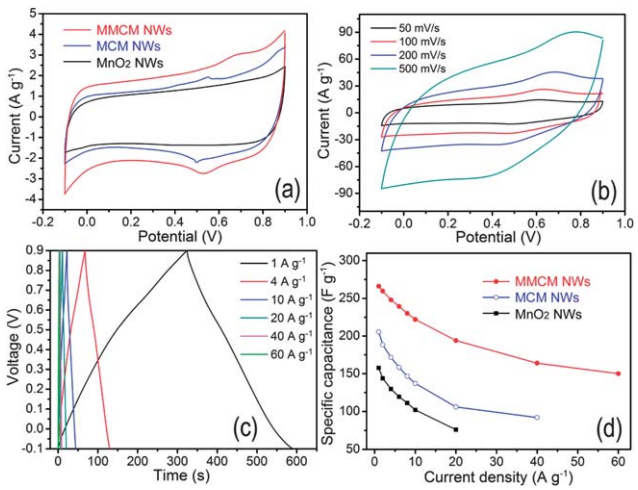

Fig. 5 (a) CV curves at a scan rate of 10 mV s^{-1} and (d) the specific capacitance as a function of different current densities of the MMCM hybrid nanowires (red lines), the MCM hybrid nanowires (blue lines) and the pristine MnO_2 nanowires (black lines). (b) CV curves at 50–500 mV s^{-1} and (c) charge–discharge curves at 1–60 A g^{-1} of the MMCM hybrid nanowires.

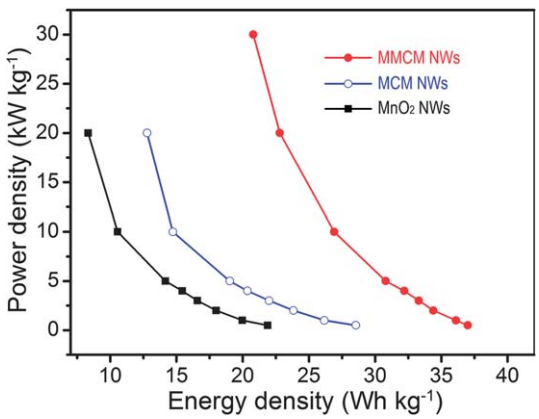

Fig. 6 Ragone plot (power density *vs.* energy density) of the MMCM hybrid nanowires (red line), the MCM hybrid nanowire (blue line) and the pristine MnO_2 nanowires (black line), respectively. The energy densities and power densities were derived from the charge–discharge curves at different current densities.

of 30 kW kg^{-1}, the energy density was still estimated to be 20.8 W h kg^{-1}. At a lower power density, the energy density reaches as high as 37.0 W h kg^{-1}. Such energy and power performance is significantly better than that of the current electrochemical capacitors reported in recent literature.[17,39,41] The present results have shown that the MMCM hybrid nanowire developed here is a very promising electrode material for high performance supercapacitors.

The long-term cycle stability of electrode materials is a critical requirement for practical applications. Fig. 7 shows the CV curves and the specific capacitance as a function of cycle number at a scan rate of 50 mV s^{-1} for 1200 cycles. It can be seen that all the CV curves are almost overlapping with each other, suggesting a good cycling stability. The specific capacitance increases slightly in the first 200 cycles and then remains almost constant. A similar improvement of the specific capacitance upon cycling has also been reported for other manganese oxide-based electrode materials.[42,43] The increase of the specific capacitance may be due to the activation effect of electrochemical cycling.[42] After the cycling test, the electrolyte remained transparent, indicating minimal dissolution of active materials into the solution, which is the main cause of specific capacitance loss in manganese oxide-based capacitors.[44,45] The carbon shells protected the manganese oxide from dissolving in electrolyte to some extent. Therefore, the cycling stability of our hybrid material is superior to the pure MnO_2,[40] and MnO_2-based composites.[22] The results confirmed that the as-synthesized hybrid nanowires exhibit an outstanding electrochemical stability.

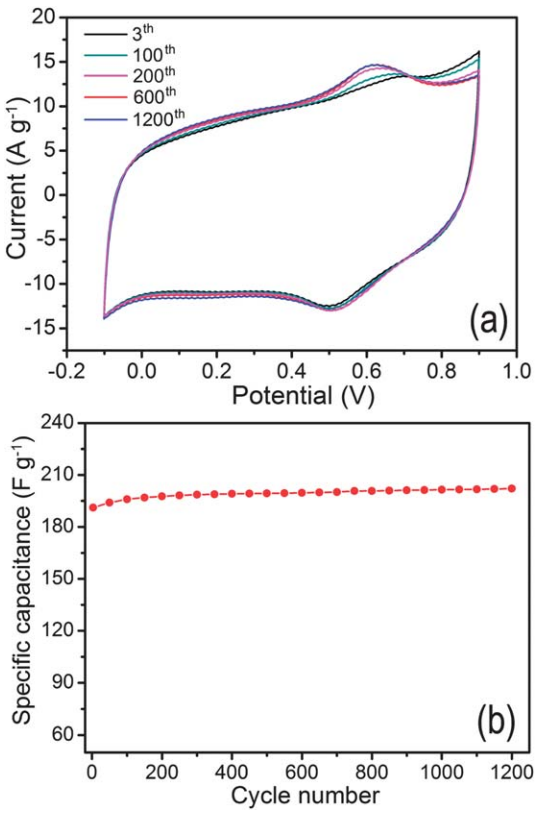

Fig. 7 (a) CV curves of cycles 3 to 1200 and (b) the specific capacitance as a function of cycle number at 50 mV s^{-1} of the MMCM hybrid nanowires.

On top of the advantage and good results discussed earlier, it is noted that optimization of the hybrid materials is another essential consideration for high capacitance performance. In the present work, we aim to control the thickness of the carbon layer, thus optimizing the material by tuning dopamine concentration. The carbon content in the hybrids was determined by TGA (Fig. S4, ESI†), and the specific capacitances of these hybrid nanowires are listed in Table 1. The corresponding CV and charge–discharge curves of the different carbon content electrodes can be found in the ESI†. Among them, the MMCM hybrid nanowires with 50.6% carbon content exhibit the highest specific capacitance. The hybrid nanostructure not only takes full advantage of the electrical double layer capacitance from the carbon layer, but also the pseudocapacitance from manganese oxide embedded inside. Moreover, the hybrid electrodes consistently show higher specific capacitance than that of the pristine manganese oxide electrode, further indicating that the carbon layer indeed facilitates the harvest of the manganese oxide pseudocapacitance and the synergetic effect of both components.

The results above have shown that the present MMCM hybrid nanowires exhibit excellent electrochemical properties and high cycling stability. These, in turn, have made them a very promising electrode material for high performance supercapacitors. As mentioned earlier, the unique hybrid materials have several advantages. Detailed speaking, firstly, to improve the poor conductivity of metal oxides, the manganeseoxide nanowires were fully and uniformly covered by a layer of mesoporous carbon with good electrical conductivity. This made the hybrid materials behaved just as "carbon materials", and each nanowire has made contact between the carbon layers. During the carbonization process, it is easy for this one dimensional MMCM hybrid nanostructure to form a network, which could greatly improve the conductivity of the electrode. Furthermore, the loading manganese oxide nanoparticles on the surface of mesoporous carbon can be almost fully utilized due to their small size. In such a hybrid configuration, manganese oxide offers the desired high specific capacitance, and the highly graphitic carbon-tipped mesoporous carbon allows fast ion diffusion into the core manganese oxide. Secondly, the porous nature of the system has facilitated high surface area, and uniform pore size distribution. These properties have allowed a higher rate of solution infiltration and facilitated the ions insertion/extraction and electrons transport, freely in the electrode. Combining one-dimensional nanostructures, the hybrid material further shortens the effective diffusion path in the hybrid nanowire. At the same time, the mesoporous carbon shell, with much higher electrical conductivity than that of manganese oxide, serves as a conducting pathway for the transport of electrons, and also acts as a buffer to alleviate the volume expansion caused by repeated

Table 1 Specific capacitance of the pristine MnO_2 nanowires and the MMCM hybrid nanowires with different carbon content

Specific capacitance value (F g^{-1})	The pristine MnO_2 nanowires	The MMCM hybrids with different carbon content		
		30.5 wt%	50.6 wt%	69.3 wt%
At 10 mV s^{-1}	130	195	226	130
At 1 A g^{-1}	157	216	266	170

ionic intercalation. A schematic representation has been illustrated in Fig. 1. This configuration ensured an effective utilization of the core manganese oxide with the assistance of highly graphitic carbon-tipped mesoporous carbon, and then resulted in an excellent electrochemical performance, *i.e.* high specific capacitance, even at a high scan rate or a high current density. Thirdly, the highly graphitic carbon tipped feature has further prompted an excellent rate capability of this hybrid nanostructure. They showed excellent conductivity due to the high graphitization degree. More importantly, highly graphitic carbon could deliver the stored energy under a high current density, since its specific capacitance was almost independent on current density.[30,46] Finally, this novel hybrid nanostructure is really close to the requirements of practical applications due to its low cost and high concentration of manganese oxide, while maintaining a considerable specific capacitance and an excellent rate capability. The simple synthesis method is realizable. It is believed that the present study provides a new route to design high performance supercapacitors materials and can be extended to the synthesis of other transition metal oxide based hybrid materials.

Conclusions

In conclusion, a new route has been reported to tackle the potential problems, such as poor conductivity, of transition metal oxide as electrochemical materials in energy storage applications. With manganese oxide as an example, for the first time, we have successfully synthesized one dimensional highly graphitic carbon-tipped manganese oxide/mesoporous carbon/manganese oxide hybrid nanostructure for high performance supercapacitors applications. The hybrid materials with 50.6% carbon content exhibit a high specific surface area (137 $m^2\ g^{-1}$) and uniform pore size distribution (~3.8 nm), which lead to excellent capacitive performance. The specific capacitance of the hybrid nanowires reaches as high as 266 F g^{-1} at a current density of 1 A g^{-1}, which is about 1.7 times that of the pristine MnO_2 nanowires (157 F g^{-1}). Even at a current density of as high as 60 A g^{-1}, the specific capacitance still remains at 150 F g^{-1}, about 56.4% capacity retention. The energy density is estimated to be as high as 20.8 W h kg^{-1} at a power density of 30 kW kg^{-1}. Supercapacitors based on this novel hybrid nanomaterial are of low cost with high performance and would accelerate their adoption in practical application.

Acknowledgements

This work was supported by the National Natural Science Foundation of China (20925621), the Program of Shanghai Subject Chief Scientist (08XD1401500), and the Shanghai Shuguang Scholars Tracking Program (08GG09). The authors acknowledge Dr J. Yan for the valuable discussions.

Notes and references

1 A. S. Arico, P. Bruce, B. Scrosati, J.-M. Tarascon and W. V. Schalkwijk, *Nat. Mater.*, 2005, **4**, 366.
2 M. Winter and R. J. Brodd, *Chem. Rev.*, 2004, **104**, 4245.
3 P. J. Hall, M. Mirzaeian, S. I. Fletcher, F. B. Sillars, A. J. R. Rennie, G. O. Shitta-Bey, G. Wilson, A. Cruden and R. Carer, *Energy Environ. Sci.*, 2010, **3**, 1238.
4 J. R. Miller and P. Simon, *Science*, 2008, **321**, 651.
5 H. Zhang, G. P. Cao, Z. Y. Wang, Y. S. Yang, Z. J. Shi and Z. N. Gu, *Nano Lett.*, 2008, **8**, 2664.
6 H. L. Wang, H. S. Casalongue, Y. Y. Liang and H. J. Dai, *J. Am. Chem. Soc.*, 2010, **132**, 7472.
7 C. C. Hu, K. H. Chang, M. C. Lin and Y. T. Wu, *Nano Lett.*, 2006, **6**, 2690.
8 H. Jiang, T. Zhao, C. Z. Li and J. Ma, *J. Mater. Chem.*, 2011, **21**, 3818.
9 R. K. Paul, M. Ghazinejad, M. Penchev, J. Lin, M. Ozkan and C. S. Ozkan, *Small*, 2010, **6**, 2309.
10 E. Raymundo-Piñero, F. Leroux and F. Béguin, *Adv. Func. Mater.*, 2006, **18**, 1877.
11 K. Wang, J. Y. Huang and Z. X. Wei, *J. Phys. Chem. C*, 2010, **114**, 8062.
12 C. P. Fonseca, J. E. Benedetti and S. Neves, *J. Power Sources*, 2006, **158**, 789.
13 L. Espinal, S. L. Suib and J. F. Rusling, *J. Am. Chem. Soc.*, 2004, **126**, 7676.
14 H. Jiang, T. Zhao, J. Ma, C. Y. Yan and C. Z. Li, *Nanoscale*, 2010, **2**, 2195.
15 A. Débart, A. J. Paterson, J. Bao and P. G. Bruce, *Angew. Chem., Int. Ed.*, 2008, **47**, 4521.
16 T. Shinomiya, V. Gupta and N. Miura, *Electrochim. Acta*, 2006, **51**, 4412.
17 R. Liu and S. B. Lee, *J. Am. Chem. Soc.*, 2008, **130**, 2942.
18 S. J. Guo, S. J. Dong and E. K. Wang, *Small*, 2008, **4**, 1133.
19 H. B. Zeng, W. P. Cai, Y. Li, J. L. Hu and P. S. Liu, *J. Phys. Chem. B*, 2005, **109**, 18260.
20 H. Jiang, T. Zhao, J. Ma, C. Y. Yan and C. Z. Li, *Chem. Commun.*, 2011, **47**, 1264.
21 S. R. Sivakkumar, J. M. Ko, D. Y. Kim, B. C. Kim and G. G. Wallace, *Electrochim. Acta*, 2007, **52**, 7377.
22 R. Liu, J. Duay and S. B. Lee, *ACS Nano*, 2010, **4**, 4299.
23 A. L. M. Reddy, M. M. Shaijumon, S. R. Gowda and P. M. Ajayan, *Nano Lett.*, 2009, **9**, 1002.
24 S. W. Lee, J. Kim, S. Chen, P. T. Hammond and Y. Shao-Horn, *ACS Nano*, 2010, **4**, 3889.
25 Y. Hou, Y. W. Cheng, T. Hobson and J. Liu, *Nano Lett.*, 2010, **10**, 2727.
26 W. Chen, Z. L. Fan, L. Gu, X. H. Bao and C. L. Wang, *Chem. Commun.*, 2010, **46**, 3905.
27 A. E. Fisher, K. A. Pettigrew, D. R. Rolison, R. M. Stroud and J. W. Long, *Nano Lett.*, 2007, **7**, 281.
28 J. Yan, Z. J. Fan, T. Wei, J. Cheng, B. Shao, K. Wang, L. P. Song and M. L. Zhang, *J. Power Sources*, 2009, **194**, 1202.
29 Y. Wang, H. Xia and J. Y. Lin, *ACS Nano*, 2010, **4**, 1425.
30 L. L. Zhang, R. Zhou and X. S. Zhao, *J. Mater. Chem.*, 2010, **20**, 5983.
31 M. E. Plonska-Brzezinska, A. Palkar, K. Winkler and L. Echegoyen, *Electrochem. Solid-State Lett.*, 2010, **13**, K35.
32 H. Lee, S. M. Dellatore, W. M. Miller and P. B. Messersmith, *Science*, 2007, **318**, 426.
33 W. Chen, N. Wang, L. Liu, Y. R. Cui, X. Cao, Q. J. Chen and L. Guo, *Nanotechnology*, 2009, **20**, 445601.
34 J. Q. Hu, R. J. Zou, Y. G. Sun and Z. G. Chen, *J. Phys. Chem. C*, 2010, **114**, 8282.
35 A. Vinu, D. P. Sawant, K. Ariga, M. Hartmann and S. B. Halligudi, *Microporous Mesoporous Mater.*, 2005, **80**, 195.
36 M. W. Xu, L. B. Kong, W. J. Zhou and H. L. Li, *J. Phys. Chem. C*, 2007, **111**, 19141.
37 R. R. Jiang, T. Huang, Y. Tang, J. L. Liu, L. G. Xue, J. H. Zhuang and A. S. Yu, *Electrochim. Acta*, 2009, **54**, 7173.
38 T. Bordjiba and D. Belanger, *J. Electrochem. Soc.*, 2009, **156**, A378.
39 S. Chen, J. W. Zhu, X. D. Wu, Q. F. Han and X. Wang, *ACS Nano*, 2010, **4**, 2822.
40 J. W. Liu, J. Essner and J. Li, *Chem. Mater.*, 2010, **22**, 5022.
41 Z. Chen, Y. C. Qin, D. Weng, Q. F. Xiao, Y. T. Peng, X. L. Wang, H. X. Li, F. Wei and Y. F. Lu, *Adv. Funct. Mater.*, 2009, **19**, 3420.
42 Y. Dai, K. Wang and J. Y. Xie, *Appl. Phys. Lett.*, 2007, **90**, 104012.
43 M. Toupin, T. Brousse and D. Bélanger, *Chem. Mater.*, 2002, **14**, 3946.
44 S. C. Pang, M. A. Anderson and T. W. Chapman, *J. Electrochem. Soc.*, 2000, **147**, 444.
45 J. Yan, E. Khoo, A. Sumboja and P. S. Lee, *ACS Nano*, 2010, **4**, 4247.
46 C. Portet, G. Yushin and Y. Gogotsi, *Carbon*, 2007, **45**, 2511.